EPJ Web of Conferences **17**, 16002 (2011)
DOI: 10.1051/epjconf/20111716002

Scattering of ^{9}Li on ^{208}Pb at energies around the Coulomb barrier

M. Cubero[12,a], J. P. Fernández-Garcia[3], J. A. Lay[3], L. Acosta[4], M. Alcorta[1], M. Madurga[1], M. A. G. Alvarez[3], M. J. G. Borge[1], L. Buchmann[6], C. A. Diget[7], B. Fulton[7], H. O. U. Fynbo[8], D. Galaviz[9], J. Gómez-Camacho[5], I. Martel[4], A. Moro[3], I. Mukha[10], T. Nilsson[11], A. M. Sánchez-Benítez[4], A. Shotter[6], O. Tengblad[1], and P. Walden[6]

[1] Instituto de Estructura de la Materia, CSIC, E-28006 Madrid, Spain.
[2] CICANUM, Universidad de Costa Rica, Apdo. 2060, San José, Costa Rica.
[3] Dpto Física Atómica Molecular y Nuclear, Facultad CC Físicas, Universidad de Sevilla, Aptdo. 1065, 41080 Spain.
[4] Dpto de Física Aplicada, Universidad de Huelva, E-21071 Huelva, Spain.
[5] Centro Nacional de Aceleradores, E-41092-Sevilla, Spain.
[6] TRIUMF, V6T2A3 Vancouver B.C., Canada.
[7] Department of Physics, University of York, YO10 5DD Heslington, York, U.K.
[8] Department of Physics and Astronomy, University of Aarhus, DK-8000, Århus, Denmark.
[9] Centro de Física Nuclear da Universidade de Lisboa, 1649-003 Lisbon, Portugal.
[10] Instituto de Física Corpuscular, CSIC-Universidad de Valencia, Spain.
[11] Fundamental Physics, Chalmers University of Technology, S-41296 Göteborg, Sweden.

Abstract. In order to study the dynamics of ^{11}Li and ^{9}Li beams in a strong electric field at energies around the Coulomb barrier, we measured at the ISACII-TRIUMF Facility the angular distribution of elastic and inelastic scattering of ^{11}Li+^{208}Pb at 24.2 and 29.7 MeV and ^{9}Li+^{208}Pb at 24, 29.5 and 33 MeV laboratory energies. We present here the first determination of the angular distribution of the cross section of ^{9}Li+^{208}Pb. The results are compared with theoretical calculations using the double-folding São Paulo Potential (SPP) for the real part and for the imaginary part a Woods-Saxon potential. A good overall agreement is obtained.

1 Introduction

The neutron-rich lithium isotope ^{11}Li is the archetype of a borromean halo nucleus with a half-live of 8.5(2) ms [1], and structurally is composed of a ^{9}Li core and two weakly bound neutrons with S_{2n}=369.15(65) keV [2]. Due to the loosely bound structure, the neutron halo should be easily polarizable in the strong electric field of a heavy target such as ^{208}Pb.

The size of ^{11}Li is abnormally big. The rms matter radius for the Li isotopes with A from 6 to 9 is around 2.45 fm, but for A=11 the rms radius is 3.71(2) fm [3].

Therefore it is interesting to study the dynamic of the halo nucleus ^{11}Li at Coulomb barrier energies on the intense electric field created by a ^{208}Pb target. This process can reveal new features of halo nuclei as predicted by [4]. For halo nuclei it is expected that collisions with heavy targets, in our case ^{208}Pb, at energies below the Coulomb barrier will depart from Rutherford scattering. This deviation can shed light on the structure of the ^{11}Li nucleus as well as give a hint on how the scattering process depends on the coupling to the continuum. Two effects are explored: First, the Coulomb break-up process will compete and reduce the elastic cross section. Secondly, the distortion of the wave function generated by the displacement of the charged core with respect to the center of mass of the nucleus should reduce the Coulomb repulsion, and thus the elastic cross sections [4].

^{9}Li is an exotic nucleus with a half-live of 178.3(4) ms [5], a ground state with a spin-parity $J^{\pi}=\frac{3}{2}^{-}$ and a matter radius of 2.45(3) fm [3]. The magnetic and quadrupole moments were reported in [5,6]. The most recent values for the ground state are μ = +3.43678(6)μ_N and Q_{exp} = -30.6(2) mb [6].

The first known excited state of ^{9}Li is $J^{\pi}=\frac{1}{2}^{-}$ with an excitation energy of 2691(5) keV. The next known state is a $(\frac{5}{2}^{-})$ resonance at 4296(15) keV excitation energy. There are experimental evidences of two more states with excitation energies of 5380(60) and 6430(15) keV [5]. Theoretical calculations for ^{9}Li states have been presented [7–10]. The recently *ab initio* no-core shell model (NCSM) calculations [10] provide E2 transition matrix elements for states with $J^{\pi}=\frac{5}{2}^{-}$ and $\frac{7}{2}^{-}$, but these transition probabilities have not been measured yet. For the reaction ^{9}Li+^{208}Pb there are two breakup/transfer channels [11]. The first, produces ^{7}Li+^{210}Pb (Q = +3.0 MeV). The second, ^{8}Li+^{209}Pb (Q = -0.1 MeV). Another possibility [11] is the breakup of ^{9}Li on two charged fragments ^{4}H+^{5}He (Q = -2.4 MeV).

In order to disentangle the contribution of the loosely bound structure of ^{11}Li to the reaction process, one should know the behavior of the core, ^{9}Li, in the same conditions. Previously, the cross section of ^{9}Li on a 0.3 mg·cm^{-2}

[a] e-mail: m.cubero@csic.es

thick ^{208}Pb target has been measured at 86 MeV and the results have been compared to different calculations [12]. This energy is high compared with the Coulomb barrier at CM ($V_B \sim 30$ MeV) for the ^{9}Li + ^{208}Pb system. Near the Coulomb barrier, the fusion cross section of ^{9}Li + ^{208}Pb has been measured at CM energies from 23.9 to 43.0 MeV, the "reduced" fusion excitation function was found to be equivalent for the A=7-9 Li isotopes [11]. Due to the lack of information on the ^{9}Li scattering on lead around the Coulomb barrier we decided to study this process in detail to characterize the potential parameters describing the dynamic behavior of the ^{11}Li core, ^{9}Li. The results of this work are presented herein.

2 Experiment

The experiment was performed in ISAC-II facility at TRIUMF. The cross section of ^{11}Li on ^{208}Pb at laboratory energies of 24.2 and 29.7 MeV was measured. Further, in order to characterize the Optical Potential (OP) parameters for this system we measured the ^{9}Li + ^{208}Pb scattering, at the same center of mass energies as well as at an energy well beyond the Coulomb barrier.

Both secondary beams of ^{9}Li and ^{11}Li were produced with a primary 100 μA proton beam of 500 MeV [13] from the cyclotron TRIUMF and Ta primary target. The secondary beams were transported to the ISAC-II facility for post acceleration. The time duration of each measurement is given in Table 1. The average yield with the ^{11}Li beam as detected in our circular Si monitor detector (thickness of 700 μm and active area of 300 mm^2) placed in the beam axis after the ^{208}Pb scattering target was 4.300 ^{11}Li/s with a maximum yield approaching 6.000 pps.

In order to identify all the fragments in the relevant angular range, we designed and optimized the configuration of the setup by calculating the losses of energy on ΔE and E sensitive parts of the telescopes for both the ^{9}Li (breakup) and ^{11}Li (elastic) for different incoming energies. Our setup consisted of four telescopes as illustrated in Fig. 1. In the forward direction we put two telescopes, T1 and T2, each one consisting of a Double-Sided Silicon Strips Detector (DSSSD) [14, 15] of 16x16 strips with 40 μm thick ΔE detector and 500 μm thick PAD E detector. Both detectors were at 80 mm from the target covering different angles T1:10-40° and T2:30-60°. The backward

Table 1. Summary of the experimental conditions used at TRIUMF to study the dynamics of the ^{11}Li + ^{208}Pb and ^{9}Li + ^{208}Pb systems. The different energies, target thicknesses and time duration are indicated.

Beam	Energy (MeV·u^{-1})	Target (mg·cm^{-2})	Energy (MeV) @ Mid-Target	Time (h)
^{9}Li	2.67	1.45	23.77	11.75
^{9}Li	3.27	1.45	29.20	7.63
^{9}Li	3.27	1.90	29.12	9.95
^{9}Li	3.67	1.90	32.77	31.05
^{11}Li	2.2	1.45	24.18	82.20
^{11}Li	2.7	1.45	29.68	118.12

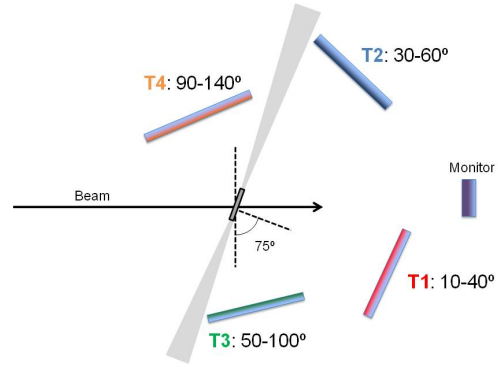

Fig. 1. (Color online). Schematic view of the experimental setup. The positions of the Pb, monitor detector, forward (T1, T2) and backward (T3, T4) telescopes are shown. The shadow of the target in is gray color.

telescopes T3 and T4 consisted of a 20 μm thick ΔE Single-Sided Silicon Strip Detector (SSSD) [14, 15] of 16 strips in front of a 60 μm thick E DSSSD.

For the T3 and T4 telescopes the detector center was chosen at a distance of 52 mm from the beam-target intersection, covering the following angles, T3:50-100° and T4:90-140°.

The segmentation of each the detector system gave rise to 256 pixels (16x16 strips) by matching front and back strips of the DSSSD, resulting in a high angular resolution. Due to the different distances between telescope and target the angular resolution is 2-3° for T1 and T2 and for the rear detectors (T3 and T4) between 3-4°.

The choice of the angles covered by the telescopes was made considering the behavior expected for the differential cross section for the elastic scattering of the halo nucleus ^{11}Li, according to the coupled-channels calculation developed by us which includes both nuclear and Coulomb couplings to the continuum. We used two targets of ^{208}Pb with thicknesses of 1.45 and 1.9 mg·cm^{-2}, both tilted at 75° with respect to the beam axis. The kinematic channels for the elastic, transfer and break-up fragments of ^{11}Li on a 1.45 mg·cm^{-2} thick ^{208}Pb tilted target is shown in Fig. 2.

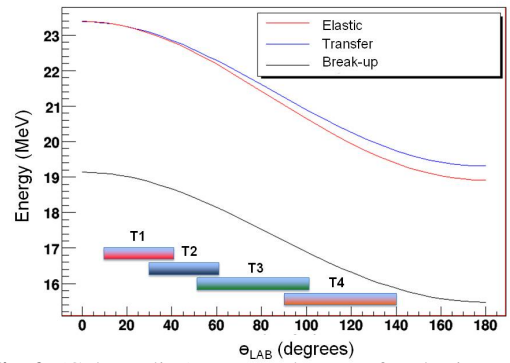

Fig. 2. (Color online). Expected energy for elastic and break-up reaction fragments in the four telescopes for a ^{11}Li beam at 24.7 MeV on a target of 1.45 mg·cm^{-2}.

3 Experimental Analysis

We present here the first determination of the angular distribution for the ^{9}Li cross section on lead at energies around the Coulomb barrier. The experimental results are analyzed in the framework of the optical model (OM) and also using a coupled channel (CC) analysis.

Due to the long duration of the data taking, the stability of the electronics was checked by looking at the centroid of the peaks obtained with the calibration *alpha*-sources as well as those of the pulse signal. The dead time of the system and the possible differences between telescopes were studied by integrating the pulser peak area in different files. We confirmed that no electronic change occurred during the data taking. In the experimental analysis the relevant events were selected in the following way. We included an individual threshold for each strip. Furthermore, when two neighbor strips were fired the event was disregarded to avoid charge sharing [14, 15]. The strip energy calibrations were performed using ^{148}Gd and the triple-α source (^{239}Pu + ^{241}Am + ^{244}Cm). To separate well the signal from heavy ions and avoid beta contributions, a condition in the energy deposited in the front and back strips forming the pixel was applied, $\Delta E_{diff} \leq$70 keV. There was a small percentage of events of multiplicity two that hit the same front or back strip. These events do not pass the energy matching condition although they were good physical events, so they were rescued and treated individually.

Elastic events were selected in the two-dimensional plot of ΔE versus total E mass spectra. A clear identification of the elastic peaks, both in the ^{9}Li and in the ^{11}Li scattering data were achieved. A preliminary data analysis was done assuming that the detectors T1 and T2 were at the position determined by the geometrical measurements, and the optical beam axis centered in the ^{208}Pb target. The solid angle was calculated for each pixel, considering that it depends on the laboratory angle and the projection of the pixel area (3x3 mm^2) over a tangent sphere centered in the target. Due to the close geometry of the setup, a refined study of the angle subtended by each pixel was done based on the expected flat behavior of the ratio of the elastic cross section divided by Rutherford at forward angles. This correction includes the losses for the events arriving in between strips. The optimization for the position of the T1 and T2 telescopes was performed by the χ^2 minimization of the Rutherford angular dependence for the ^{9}Li data at 2.67 MeV·u^{-1}. The differential cross section with optimized position vectors for each detector was calculated by the weighted average of the pixels corresponding to a certain angle. The angles covered by the T3 and T4 telescopes were determined only by geometrical considerations as angular dependence of the cross section get flatter. For angles larger than 60° the pixels of one strip corresponds to the same angular interval. Three strips of ΔE3 SSSD detector were not working. Furthermore the target frame shadowed a bit the larger angles in the telescopes T2 and T3, reduced the overlap between T2 and T3 and contributed to a region without angular coverage between T3 and T4, Fig. 3.

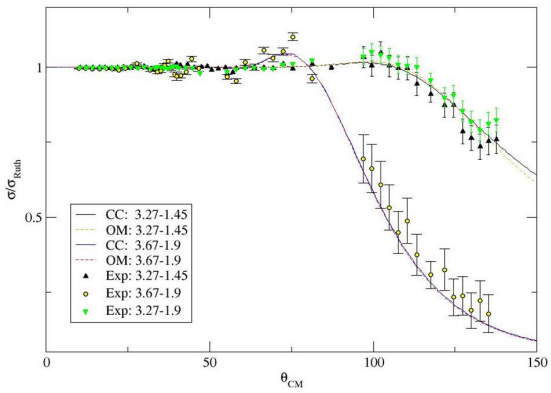

Fig. 3. Differential cross section divided by Rutherford is shown for ^{9}Li on ^{208}Pb at 29.5 and 33 MeV beam energies. Experimental data at 29.5 MeV is given for the two measured targets of 1.45 mg·cm^{-2} (black up triangles) and 1.9 mg·cm^{-2} (green down triangles). The OM calculations correspond to the dashed lines. Solid lines represent the CC calculations. The fitting parameters are shown in Table 2. Both, the OM and CC calculations reproduce similarly well the data.

4 Interpretation of the Results

The measured elastic data have been analyzed within the framework of the optical model, using the FRESCO code [16, 17]. The ^{9}Li scattering data at 24 MeV were excluded from this analysis since these data are very close to Rutherford cross section and hence they showed very little sensitivity with respect to the parameters of the nuclear potential. In this analysis, the real part of the ^{9}Li+^{208}Pb interaction was described in terms of the double-folding São Paulo potential (SPP) [18] with the ^{9}Li matter radius of R_{rms} = 2.45(3) fm from Ref. [3] and matter radius for ^{208}Pb obtained from a Hartree-Fock calculation, giving R_{rms} = 5.53 fm. The imaginary part was parametrized using a Woods-Saxon potential. The three parameters (W_i, r_i and a_i) of the Woods-Saxon potential as well as the normalization of the real part (N_r) were taken as adjustable parameters in order to reproduce the experimental data. In a first approach, we searched for a set of parameters that gave the best overall fit to the ^{9}Li scattering data at 29.5 and 33 MeV. For the former case, we considered the data for the 1.45 and 1.9 mg·cm^{-2} targets together. This provided the geometry parameters r_i = 1.35 fm and a_i = 0.51 fm. Then, we kept the geometry fixed and readjusted the normalization N_r and the imaginary depth W_i at each energy. The resulting parameters are listed in Table 2 and the corresponding angular distributions are compared with the data in Fig. 3. We can see that it is possible to describe the

Table 2. The parameters used in the OM and CC calculations are listed. The parameters r_i = 1.35 fm and a_i = 0.51 fm are equal in all cases.

Model	Energy (MeV/u)	N_r	W_i(MeV)	χ^2/n
OM	3.27	0.883	6.01	4.1
OM	3.67	0.798	17.6	6.4
CC	3.27	0.85	6.50	4.2
CC	3.67	0.95	17.18	6.2

data at both energies using a fixed geometry. The real normalization constants are slightly smaller than unity, what would indicate some attractive polarization effect due to the coupling with non-elastic channels. From the values quoted in Table 2 we can see also that the data at 29.5 MeV requires a significantly smaller imaginary potential depth, which is an expected result due to the progressive closure of non-elastic channels when the incident energy decreases into the region of sub-Coulomb energies.

In addition, we have studied the effect of the coupling to the first excited state of ^{9}Li on the elastic cross section. For this purpose, we have performed CC calculations in which the ground and first excited states of ^{9}Li are coupled. We assume a collective model for these states. Since the ^{9}Li has a sizable quadrupole moment, we have also taken into account the reorientation term for the ground state. The strength of the quadrupole coupling potential arising from the Coulomb interaction is given by the reduced matrix element of the electric operator, M(E2; $J_i \rightarrow J_f$). For the $3/2^- \rightarrow 1/2^-$ coupling, we used the reduced matrix element M(E2; $3/2^- \rightarrow 1/2^-$) = 3.55 e·fm^2, which was obtained from the transition probability B(E2; $3/2^- \rightarrow 1/2^-$) = 3.15 e^{2}fm^4 given in [7]. For the reorientation term, the reduced matrix element, M(E2), was obtained from the experimental quadrupole moment, Q_{exp} = -27.4(1) mb [5], giving M(E2; $3/2^- \rightarrow 3/2^-$) = -3.86 e·fm^2.

The radial part of the nuclear coupling was obtained as the derivative of the central potential multiplied by the reduced deformation length, $\delta_{if} \equiv \langle J_f \| \hat{\delta}_2 \| J_i \rangle$. For each transition we first determined a Coulomb deformation length as,

$$\delta^C_{ij} = \langle J_f \| \hat{\delta}^C_2 \| J_i \rangle = M(E2; J_i \rightarrow J_f) \frac{4\pi}{2ZR} \qquad (1)$$

where $Z = 3$ is the charge number of ^{9}Li and R $\simeq$ 3.16 fm is the radius derived from R $\simeq$ R$_{rms} \cdot \sqrt{\frac{5}{3}}$. Then, assuming that the Coulomb and charge distributions have the same deformation lengths, we estimated the nuclear deformation lengths as $\delta^N_{if} \approx \delta^C_{if}$.

For the *bare* projectile-target interaction, we used the same prescription as for the OM analysis, with the real part given by the SPP potential and the imaginary part parametrized in terms of a Woods-Saxon potential. For the latter, the parameters r_i and a_i were fixed to the values found in the OM analysis. The normalization of the real part and the depth of the imaginary part were fitted in order to reproduce the 29.5 and 33 MeV scattering data. The extracted values are given in Table 2. These parameters are close to those found in the OM analysis, indicating that the elastic cross section is only weakly affected by the couplings included in the CC analysis. This is also observed in the calculated angular distributions shown in Fig. 3, where the OM and CC calculations are almost indistinguishable.

This analysis should be considered as preliminary, since both the experimental and theoretical analysis are in progress [19]. A more detailed analysis will be presented elsewhere [20].

5 Summary and Outlook

The elastic scattering of a exotic ^{9}Li beam on a ^{208}Pb target has been measured at three energies: 24, 29.5 and 33 MeV. For the lowest energy, which is below the nominal Coulomb barrier, the extracted cross section is consistent with an almost pure Rutherford scattering. For the two other energies, the measured angular distribution follows the Rutherford formula for scattering angles up to 45°. The data for these two energies have been compared with OM calculations.

A previous OM analysis of these data [19] was performed with an optical potential derived from the elastic scattering of ^{7}Li by ^{208}Pb at Coulomb barrier energies in [21]. This potential proved to be inadequate to describe the present data in spite of the trend indicated by the recent fusion results [11].

With the idea of extracting a global optical potential for the measured energies, we performed a best-fit analysis of the data starting from the above mentioned potential, fixing the geometry but allowing for the normalization of the real part and the potential depth of the imaginary part to vary.

The resulting potential provides a reasonably good overall agreement of the angular distribution for energies at 29.5 and 33 MeV. Although a more refined analysis is still to be done, this kind of potentials will be an essential ingredient for the few-body calculations that will be eventually performed for the ^{11}Li+^{208}Pb elastic and breakup data measured in the same experiment.

Acknowledgments

We thank the TRIUMF and, in particular, the accelerator staff for their support during the experiment. We acknowledge support from CICYT via contract FPA2009-07387, FPA2009-08848, FPA2010-22131-C02-01 and FPA2009-07653. One of us (M.C.) acknowledges the support of the CSIC-Costa Rica fellowship program.

References

1. F. Ajzenberg-Selove etal,Nucl.Phys. A **506**, (1990) 1-158.
2. M. Smith et al., Phys. Rev. Lett. **101**, (2008) 1-4.
3. A.V. Dobrovolsky et al., Nucl. Phys. A **766**,(2006)1-24.
4. M.V. Andrés et al., Phys.Rev.Lett.**82**,(1999)1387-1390.
5. D. R. Tilley et al., Nuc. Phys. A. **745**, (2004) 155-362.
6. D. Borremans et al., Phys. Rev. C **72**, (2005) 044309.
7. P. Descouvemont, Nuc. Phys. A. **626**, (1997) 647-668.
8. P. Navrátil, Phys. Rev. C **57**, (1998) 3119-3128.
9. C. Frossén, Phys. Rev. C **79**, (2009) 021303(R).
10. A. F. Lisetskiy et al., Phys. Rev. C **80**, (2009) 024315.
11. A. Vinodkumar et al., Phys. Rev. C **80**, (2009) 054609.
12. N. K. Skobelev et al., Z. Phys **341**, (1992) 315-318.
13. G. C. Ball et al., J. Phys. G **38**, (2011) 024003.
14. U. Bergmann et al., Nucl. Inst. and Methods A. **515**, (2003) 657-664.
15. O. Tengblad et al., Nucl. Inst. and Methods A. **525**, (2004) 458-464.
16. I. Thompson, Computer Phys. Rep. **7**, (1988) 167-210.
17. I. Thompson, *Nuclear Reactions for Astrophysics* (Cambridge, 2009) 1-466.
18. L. C. Chamon, et al., Phys. Rev. C. **66**, (2002) 014610.
19. M. Cubero et al., AIP proceedings (to be published).
20. M. Cubero et al., (in preparation).
21. I. Martel et al., Nuc. Phys. A**582**, (1995) 357-368.